Available online at www.sciencedirect.com
SCIENCE DIRECT®
Biochemical and Biophysical Research Communications 316 (2004) 244–251
BBRC
www.elsevier.com/locate/ybbrc

Cell-cycle-dependent expression of the large Ca^{2+}-activated K^+ channels in breast cancer cells

Halima Ouadid-Ahidouch,[a,b,*] Morad Roudbaraki,[a] Ahmed Ahidouch,[b,c] Philippe Delcourt,[a] and Natalia Prevarskaya[a]

[a] *Laboratoire de Physiologie Cellulaire, INSERM EMI 0228, SN3, Université des Sciences et Technologies de Lille, 59655 Villeneuve d'Ascq Cédex, France*
[b] *Laboratoire de Physiologie Cellulaire et Moléculaire, Faculté des Sciences, UPJV, Bâtiment des Minimes, 33 Rue St Leu, 8000 Amiens, France*
[c] *Laboratoire de Physiologie Animale, Université Ibnou-Zohr, Faculté des Sciences, Edakhla, Agadir, Morocco*

Received 4 December 2003

Abstract

In a previous work, we have reported that the ionic nature of the outward current recorded in MCF-7 cells was that of a K^+ current. In this study, we have identified a Ca^{2+}-activated K^+ channel not yet described in MCF-7 human breast cancer cells. In cells arrested in the early G1 (depolarized cells), increasing $[Ca^{2+}]_i$ induced both a shift in the *I–V* curve toward more negative potentials and an increase in current amplitude at negative and more at positive potential. Currents were inhibited by r-iberiotoxin (r-IbTX, 50 nM) and charybdotoxin (ChTX, 50 nM). These data indicate that human breast cancer cells express large-conductance Ca^{2+}-activated K^+ (BK) channels. BK current-density increased in cells synchronized at the end of G1, as compared with those in the early G1 phase. This increased current-density paralleled the enhancement in BK mRNA levels. Blocking BK channels with r-IbTX, ChTX or both induced a slight depolarization in cells arrested in the early G1, late G1, and S phases and accumulated cells in the S phase, but failed to induce cell proliferation. Thus, the expression of the BK channels was cell-cycle-dependent and seems to contribute more to the S phase than to the G1 phase. However, these K^+ channels did not regulate the cell proliferation because of their minor role in the membrane potential.

Keywords: Ca^{2+}-activated K^+ channels; Cell-cycle progression; Breast cancer cells

There are numerous reports showing that progression through the cell cycle is dependent on ion translocations across the plasma membrane. Thus, pharmacological blockades of K^+ channels (see, review [1]) lead to cell proliferation inhibition. Recent studies demonstrated that K^+ channel activity is also a key determinant factor for cell progression through the G1 phase of mitosis [1]. For example: Kv1.3 K^+ channels have been linked to progression through the G1 phase in T lymphocytes [2] and Kv1.1 K^+ channels in G1/S transition in oligodendrocyte progenitor cells [3]. Another link between the K^+ channels and cell cycle is indicated by the finding that the activities of some K^+ channels change cyclically as cells progress through the division cycle. An example of this is the size of a K^+ current which increased during M and G1 phases in HeLa cells [4,5]. Recently, Czarnecki et al. [6] have reported an up-regulation of I_{t0} K^+ current in quiescent cells (G0 phase) compared with proliferating GH3 pituitary cell line. Furthermore, Kv1.4 and Kv4 α-subunits are responsible for I_{t0} in GH3 cells [6].

In the breast cancer MCF-7 cell line, we and others have reported that both the control of proliferation and the cell-cycle progression depend on K^+ channel activity according to the "membrane potential" model [1,7]. Thus, the inhibition of proliferation by K^+ channel blockers is due to membrane depolarization. The MCF-7 cell line expresses a plethora of distinct ionic channels: Kv1.1 [8], hEAG [7], Kv1.3 [9], KCNK9 [10], K_{ATP} [11], and a 23 pS K^+ channel, activated by Ca^{2+} and depolarization [12]. Moreover, the expression of the

* Corresponding author. Fax: +33-3-22-82-76-44.
E-mail address: ha-sciences@u-picardie.fr (H. Ouadid-Ahidouch).

0006-291X/$ - see front matter © 2004 Elsevier Inc. All rights reserved.
doi:10.1016/j.bbrc.2004.02.041

Ca^{2+}-activated K^+ channels in MCF-7 cells has been suggested by Strobl et al. [13] and Ouadid-Ahidouch et al. [14]. However, until now, both the type and the physiological role of the Ca^{2+}-activated K^+ channels in MCF-7 cells have remained unclear.

Calcium-activated K^+ channels have historically been subdivided into three distinct classes, based on their conductances and their pharmacology. These include the large-conductance (BK) channels, which are sensitive to charybdotoxin (ChTX) and iberiotoxin (IbTX) [15,16], the intermediate-conductance (hIK or hSK4) channels, which are inhibited both by ChTX and clotrimazole [15,17], and the small-conductance (SK), apamin-sensitive (and -insensitive) K^+ channels [15]. Furthermore, a number of studies have suggested that the BK K^+ channels play a functional role in controlling arterial tone [18,19]. BK channels have also been shown to be involved in the generation and maintenance of pathological conditions such as hypertension [20,21]. Moreover, the expression of BK channels is lost during development and regained when cells proliferate in response to injury or disease [22]. Ca^{2+}-activated K^+ channels are also involved both in the activation of B lymphocytes [23] and in the regulation of the Ca^{2+}-dependent pathways in human T lymphocyte activation [24].

In this study, we demonstrate that MCF-7 cells express BK K^+ channels. The expression of the BK channel appears to be cell-cycle-dependent and seems to contribute more in the S than in the G1 phase. However, these K^+ channels did not regulate cell proliferation because of their minor role in the membrane potential.

Materials and methods

Cell culture. MCF-7 cells between passages 20 and 59 were cultured in Eagle's minimum essential medium (EMEM), supplemented with 5% fetal calf serum (FCS), 2 mM L-glutamine, and 0.06% Hepes buffer, and maintained at 37 °C in a humid atmosphere of 5% CO_2 in air.

Cell synchronization. Cells were synchronized by using protocols previously described by [7]. The cells were plated in 35 mm dishes in EMEM containing 10% FCS. After 24 h, the cells were rinsed twice with PBS and incubated with serum-free EMEM for 24 h to synchronize them in early G1.

To obtain cells progressing through the G1 phase, we replaced the serum-free-medium by EMEM with 10% FCS for 7–10 h [7]. To synchronize cells on the G1/S boundary (at the end of G1), the cells were incubated with 2 mM thymidine in EMEM with 10% FCS for 24 h at 37 °C. The treatment led to a partial synchronization, since at the end of thymidine treatment, 80% of cells were accumulated in the G1 phase [25]. The removal of thymidine allowed the cells to progress through the cell cycle, since between 6 and 7 h after the treatment, about 84% of cells were found in the S phase [7,25].

Cell-cycle distribution patterns were identified by measuring cellular DNA content using flow cytometry.

Cell proliferation assay. Cells were seeded in 24-well plates in EMEM with 5% FCS. After 24 h, the cells were treated with various agents. The medium was changed every other day. After 4 days of treatment, the cell number was determined by a colorimetric method (CellTiter 96 Aqueous Non-Radioactive Cell Proliferation Assay).

Flow cytometry. Flow cytometry assays were performed on cell populations cultured in triplicate 25-cm^2 flasks. Approximately 10^6 cells were fixed with 1 ml ice-cold 70% methanol for 30 min. After fixing, cells were pelleted by centrifugation to remove the fixatives, washed three times with phosphate-buffered saline (PBS) at 4 °C, resuspended in 100 μl PBS, treated with 100 μl ribonuclease (1 mg/ml, Sigma), and stained with propidium iodide (PI, Sigma) at a final concentration of 50 μg/ml. The stained cells were stored at 4 °C in the dark and analyzed within 2 h. The stained samples were measured on a FACScan flow cytometer (Becton–Dickinson, San Jose, CA). Data were acquired for 7000 events with a variation coefficient of less than 5%, and red fluorescence was measured using a fluorescence detector 3 (FL3) on the *X*-axis. The data were stored and analyzed using CellQuest software to assess cell-cycle distribution patterns (G0/G1, S, and G2/M phases).

Electrophysiology. For electrophysiological analysis, the cells were cultured in 35 mm petri dishes at a density of 6000 cells/cm^2. Currents and membrane potential were recorded in voltage-clamp or current-clamp mode, using an Axopatch 200 B patch-clamp amplifier (Axon Instruments, Burlingame, CA) and Labmaster hardware (Digidata 2000, Axon Instrument). PClamp software (ver. 6.03, Axon Instruments) was used to control voltage, as well as to acquire and analyze data. The whole-cell mode of the patch-clamp technique was used with 3–5 MΩ resistance borosilicate fire-polished pipettes (A-M systems, Everette, WA). Seal resistance was typically in the 10–20 GΩ range. The maximum uncompensated series resistance was <10 MΩ during whole-cell recordings, so the voltage error was <5 mV for a current amplitude of 500 pA. Recordings where series resistance resulted in errors greater than 5 mV in voltage commands were discarded. Whole-cell currents were allowed to stabilize for 5 min before K^+ currents were measured. The capacitance of the membrane was measured by voltage clamp with a voltage pulse after completion of a whole-cell patch-clamp procedure and the compensation of the electrode capacitance with electronic circuits built into the patch-clamp amplifier. Results were expressed using current-densities instead of current amplitude. The cell surface of the MCF-7 cells was thus estimated by measuring their membrane capacitance (32 ± 4 pF, $n = 90$). The voltage-dependent outward currents were recorded using the whole-cell patch-clamp technique during ramps from −120 to +60 mV, applied from a holding potential of −40 mV for 250 ms. To eliminate a possible involvement of Kv1.1 K^+ channels, all experiments were conducted in the presence of 10 nM α-dendrotoxin (α-DTX).

Cells were allowed to settle in petri dishes placed at the opening of a 250-μm-inner diameter capillary for extracellular perfusions (MSC-200, Manual Solution Changer, Bio-Logic Instruments, France). The cell under investigation was continuously superfused with control or test solutions. All electrophysiological experiments were performed at room temperature.

Solutions. External and internal solutions had the following compositions (in mM): external: NaCl 145, KCl 5, $CaCl_2$ 2, $MgCl_2$ 1, and Hepes 10 at pH 7.4 (NaOH), and osmolarity 300. Internal: KCl 150, Hepes 10, EGTA 0.1, $MgCl_2$ 2 at pH 7.2 (KOH), osmolarity 292, measured with a freezing-point depression osmometer. α-DTX, ChTX, and r-iberiotoxin (r-IbTX) (Latoxan, France) were made up in BSA 1%, Hepes 5 mM (pH 7.2). Final concentrations were obtained by appropriate dilution in an external control solution.

Free Ca^{2+} concentrations for the solution applied from the inner side of the membrane were buffered with 10 mM EGTA and calculated using Maxc Software (from Chris Patton, Hopkins Marine Station, Stanford University). For example, to produce 1 μM of free Ca^{2+} solutions with (in mM): 8.3 $CaCl_2$, 1 $MgCl_2$, and 10 EGTA were used (pH 7.2).

Statistical analysis. Results were expressed as means ± SD. Experiments were repeated at least three times. Statistical analysis was performed using GraphPad InStat Software. Student's *t* test for multiple comparisons modified by the Tukey–Kramer HSD method was used to compare treatment means with control means, and one-sided *t* tests were used to test the significance of drug blocks where $p < 0.05$.

RNA extraction and reverse transcription-polymerase chain reaction (RT-PCR). Total RNA was isolated from MCF-7 unsynchronized cells, synchronized cells in the early G1 phase, cells arrested at the end of the G1 phase, and cells accumulated in the S phase, using the guanidium thiocyanate–phenol–chloroform extraction procedure [26]. After a DNAseI (Invitrogen) treatment to eliminate genomic DNA, 2 μg of total RNA was reverse transcribed into cDNA at 42 °C, using random hexamer primers (Applied Biosystems) and MuLV reverse transcriptase (Perkin–Elmer) in a 20 μl final volume, followed by PCR. PCR was carried out on the RT-generated cDNA using a GeneAmp PCR System 2400 thermal cycler (Applied Biosystems). To detect hBK (BK) cDNAs, PCR was performed by adding 1 μl (100 ng RNA equivalents) of RT template to the following mixture (final concentrations): 50 mM KCl, 10 mM Tris–HCl (pH 8.3), 2.5 mM $MgCl_2$, 200 μM of each dNTP, 1 μM of sense and antisense primers, and 1 U AmpliTaq Gold (Perkin–Elmer) in a final volume of 25 μl. Conditions of DNA amplification included an initial denaturation step of 7 min at 95 °C and 40 cycles of 20 s at 95 °C, 20 s at 58 °C, 1 min at 72 °C, and finally 7 min at 72 °C. Half of the PCR samples were analyzed by electrophoresis on a 1.5% agarose gel and stained with ethidium bromide (0.5 μg/ml). The PCR primers used to amplify the RT-generated hBK cDNAs were designed on the basis of established GenBank sequences. Primers were synthesized by Invitrogen. The primers for hBK cDNA were: 5′-AGTACAAGTCTGCCAAC CGAGAGA-3′ (nucleotides 1901–1924, GenBank Accession No. U723767) and 5′-TCCCATTCCCGCTTGAGGTACTCAA-3′ (nucleotides 2498–2474, GenBank Accession No. U723767). The expected DNA length is 598 bp. In order to confirm the identity of the amplified products, restriction analysis was carried out on each PCR product using specific restriction enzymes.

To estimate the rate of the hBK mRNA in different phases of the cell cycle, hBK cDNA was amplified along with β-actin cDNA as an internal control. The following (+) and (−) strand oligonucleotide primers were used to amplify β-actin cDNA (227 bp): 5′-CAGAGCAAGAGAGGC ATCCT-3′ and 5′-ACGTACATGGCTGGGGTGTTGAA-3′. The duplex PCR was performed as described previously [26] and the reaction products were analyzed on a 1.5% agarose gel in a Tris–borate–EDTA buffer. The gel was stained with ethidium bromide and viewed by Gel Doc 1000 (Bio-Rad, Hercules, CA, USA). The quantity of each PCR product was determined using Molecular Analyst software (Bio-Rad). The image density of the hBK PCR product was compared with the density of co-amplified β-actin to determine the ratio of hBK mRNA expression in unsynchronized and synchronized cells. All relative values of hBK expression in synchronized cells were compared and expressed as a percent of that of unsynchronized cells.

Results

Synchronization in the early G1

To determine the relative position of the sites of arrest by serum starvation, we used flow cytometry to measure the amount of time required for cells released from a 24-h arrest by serum starvation to enter S phase. Cells released from arrest by serum starvation emerged from G0/G1 up to 36 h after the addition of serum (Table 1). In MCF-7 cells, quinidine, a K^+ channel blocker, arrests the cell cycle in the early G1 phase, since the release the cells from arrest by quinidine emerged from G0/G1 between 20 and 24 h after the drug washout [27]. Thus, serum starvation appears to prevent the progression of cells through the early G1 phase. Moreover, similar washout kinetics were observed in MCF-7 cells arrested with lovastatin, an agent which is known to arrest MCF-7 cells in early G1 [28]. Our results were similar to the latter.

Ca^{2+}-activated K^+ channels in MCF-7 cells

In a previous study, we showed that the ionic nature of the outward current recorded in MCF-7 cells was that of a K^+ current because the reversal potential was close to the K^+ equilibrium potential and completely blocked by 10 mM TEA [7,8]. In synchronized MCF-7 in the early G1 phase and under typical whole-cell recording conditions (i.e., low intracellular Ca^{2+}), the outward current components were largely carried by K^+ ions since the intracellular K^+ ion (150 mM) replacement by Cs^+ ions (150 mM) reduced the amplitude of the outward current (Figs. 1A and B). Moreover, with CsCl-based solutions, the average resting potential (measured as the 0 current potential) was -6 ± 1.5 mV, much smaller than KCl-solutions (-30 ± 2 mV, $n = 10$). It was previously suggested that the predominant K^+ channel type in MCF-7 cells was a Ca^{2+}-activated K^+ channel [12]. To characterize the Ca^{2+} and voltage-activated K^+ channels, whole-cell recordings from MCF-7 synchronized in the early G1 with pipette solutions with 10 EGTA/zero-added Ca^{2+} and free Ca^{2+} concentrations of 0.5 and 1 μM resulted in dramatic increases in current amplitude across the range of 0–60 mV and a modest increase at the negative potentials (Fig. 1C). The currents elicited with ramp voltage (−120 to +60 mV during 250 ms) show a voltage-dependent K^+ current in the control conditions which activated at 0 mV. One micromolar of $[Ca^{2+}]_i$ induced both a shift in the *I–V* curve toward more negative potentials and an increase in current amplitude at negative and more at positive potential (Fig. 1C). A similar result was obtained by increasing $[Ca^{2+}]_i$ resulting from the extracellular

Table 1
Reversible G0/G1 arrest by serum starvation

Cell-cycle phase distribution	Control ($n = 4$)	Serum starvation 24 h ($n = 4$)	SVF (5%) 6 h ($n = 4$)	SVF (5%) 16 h ($n = 4$)	SVF (5%) 36 h ($n = 4$)
G0/G1	64 ± 1.06	$93.45^{***} \pm 0.25$	$88.1^{***} \pm 0.72$	$40^{***} \pm 3.6$	66.55 ± 0.43
S	26.6 ± 0.84	$3.35^{***} \pm 0.05$	$7.26^{***} \pm 0.56$	$32.8^{**} \pm 2.5$	24.6 ± 0.9
G2/M	9.6 ± 0.7	$1.6^{***} \pm 0.02$	$2.95^{***} \pm 0.3$	$14.3^{**} \pm 1.5$	8.75 ± 0.21

The experimental group medians marked by asterisks are significantly different from the control median (***$p < 0.001$ and **$p < 0.01$).

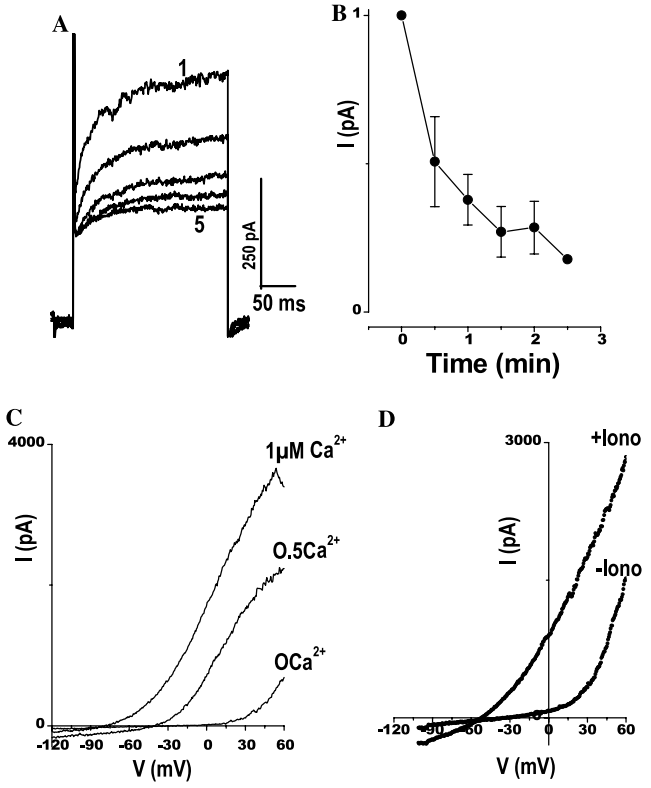

Fig. 1. Voltage-dependent currents in human breast cancer cells. (A) Representative whole-cell current traces from a single MCF-7 cell patched with CsCl-based pipette solution. The voltage-dependent current was elicited by a depolarizing voltage step from −60 to +60 mV for 250 ms; episode 1 [1]; episode 5 [5]. (B) Time courses of the decrease in the current amplitude with CsCl intracellular solution; data points are means ± SD ($n = 5$). (C) In cells arrested in early G1, application of a voltage ramp from −120 to +60 mV induced voltage-activated K^+ currents. Whole-cell current traces of three representative MCF-7 cells with estimated $[Ca^{2+}]_i$ of 0, 0.5, and 1 μM. (D) Whole current traces obtained before (− Iono) and after (+ Iono) the application of 1 μM ionomycin to the bath.

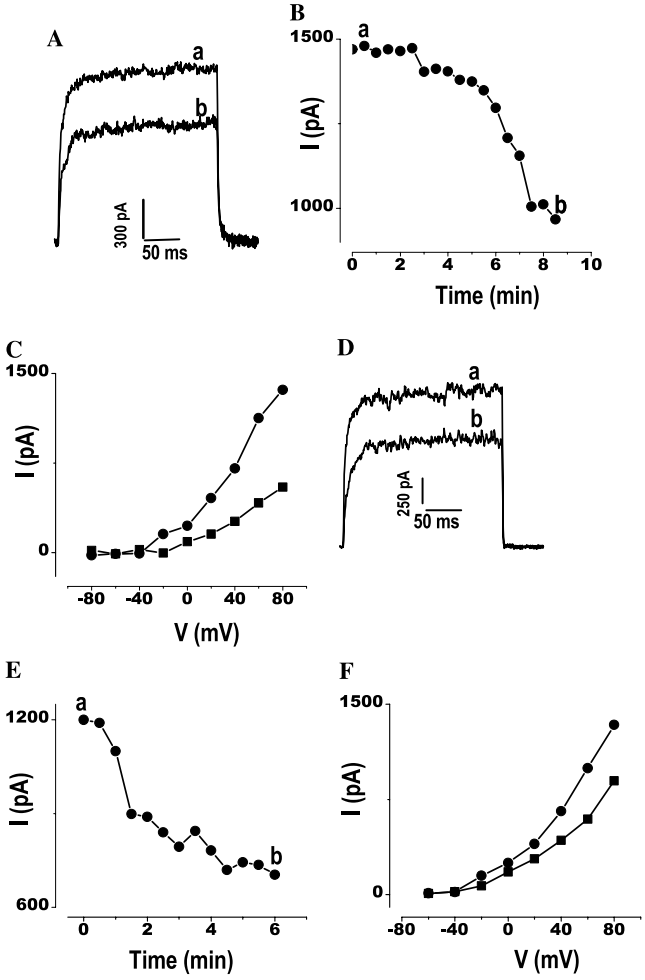

Fig. 2. Voltage-dependent currents were inhibited by the toxin-venom peptides r-iberiotoxin and charybdotoxin. (A) Examples of the K^+ currents recorded in cells arrested at the end of the G1 phase. The individual current traces were evoked by a depolarizing pulse from −60 to +80 mV for 250 ms; (a) in the control solution; (b) 5 min after the perfusion of 50 nM r-IbTX. (B) Time courses of the K^+ current recorded under control conditions and after a 50 nM r-IbTX application. (C) Current–voltage relationship in the absence (●) and presence (■) of 50 nM r-IbTX. (D) Individual current traces recorded from −60 to +80 mV for 250 ms (a) in the control solution and (b) in the presence of 50 nM ChTX. (E) Time courses of the K^+ current in the control and after a 50 nM ChTX application. (F) Current–voltage relationship in the absence (●) and presence (■) of 50 nM ChTX.

application of the Ca^{2+} ionophore ionomycin (1 μM) (Fig. 1D).

Pharmacological characterization of Ca^{2+}-activated K^+ channels in MCF-7 cells

The voltage-dependent currents in MCF-7 cells were sensitive to TEA, a well-known K^+ channel blocker. In our experiments, TEA (10 mM) reduced the whole K^+ currents by 92 ± 1.6%, with an IC_{50} of ~2 mM [7]. Thus, to identify the BK channels, we used r-IbTX and ChTX but not TEA.

In MCF-7 cells synchronized at the end of G1, we recorded a Ca^{2+}-activated current. The extracellular application of r-IbTX (50 nM), a potent inhibitor of the large-conductance K^+ channels, reduced the outward current by 52 ± 5%, $n = 15$ (Fig. 2A). The effect of r-IbTX reached a maximum at 15 ± 6 min, $n = 10$ (Fig. 2B) and was partially reversible after a 20 min washing (data not shown). The r-IbTX block was voltage-dependent (Fig. 2C). Moreover, no further significant reduction could be obtained even with 100 nM r-IbTX (60 ± 7%, $n = 10$). ChTX, an effective blocker of BK channels in several tissues [15], inhibited the macroscopic current evoked by a depolarization pulse from −60 to +80 mV (Fig. 2D). The effect of ChTX peaked at 8 ± 3.6 min ($n = 7$, Fig. 2E). In contrast to the effect of r-IbTX, the effect of ChTX was rapidly reversible (data not shown). The *I–V* curve of the ChTX-sensitive current is shown in Fig. 2F. In addition, the effects of r-IbTX and ChTX are additive ($n = 6$, data not shown).

Thus, this observation provides compelling evidence that the r-IbTX-sensitive K^+ current, under these conditions, represents about 40% of the outward current.

Comparison of the BK K^+ channel mRNA expression during the cell cycle

The expression of the BK mRNA in MCF-7 cells was studied by RT-PCR. Fig. 3A shows the results of RT-PCR analysis of the expression of BK mRNA in total RNA extracts from unsynchronized MCF-7 cells. The primers designed for BK amplified the fragment of the expected size for BK mRNA (598 bp).

In order to study the variation in BK mRNA expression during the cell cycle, we used the semi-quantitative RT-PCR as described in Materials and methods. The relative abundance of BK mRNA in different phases of the cell cycle was determined by comparing the amount of the amplification product for BK with amplification of β-actin mRNA expressed in the same sample. These experiments were conducted on the mRNA from unsynchronized MCF-7 cells, synchronized either in early or late G1, or again in the S phases of the cell cycle. The semi-quantitative RT-PCR experiments (Fig. 3B) showed that BK mRNA expression increased in cells synchronized in early G1 ($219 \pm 11\%$, $n = 4$) and at the end of the G1 ($263 \pm 23\%$, $n = 4$), when compared to unsynchronized cells. The BK mRNA expression level of the cells synchronized in the S phase tended to decrease but remained higher ($165 \pm 14\%$, $n = 4$) than the unsynchronized cells. The semi-quantitative RT-PCR experiments were performed four times on the RNAs from synchronized and unsynchronized MCF-7 cells. These experiments showed the up-regulation of the BK mRNA expression during the cell cycle, especially in early G1 and G1 of the MCF-7 cell cycle.

To determine the contribution of BK channels during the cell cycle, whole-cell patch-clamp measurements were also performed on cells arrested early in the G1 phase, at the end of the G1 phase, and in the S phase. Fig. 3C summarizes the current-density values for BK conductance. BK current-density was determined by dividing the r-IbTX-sensitive current by membrane capacitance. In fact, in cells arrested in early G1, BK-density was 8 ± 1.6 pA/pF ($n = 32$) and switched to 20 ± 1.75 pA/pF ($n = 27$, $p < 0.001$) when cells were arrested at the end of G1. BK-density decreased in cells accumulated in the S phase ($12 \pm 1{,}83$ pA/pF, $n = 30$, $p < 0.001$, Fig. 3C).

BK K^+ channels and membrane potential

We previously demonstrated that hyperpolarization may be accompanied by an increase in the number of hEAG K^+ channels and that this may be a prerequisite for

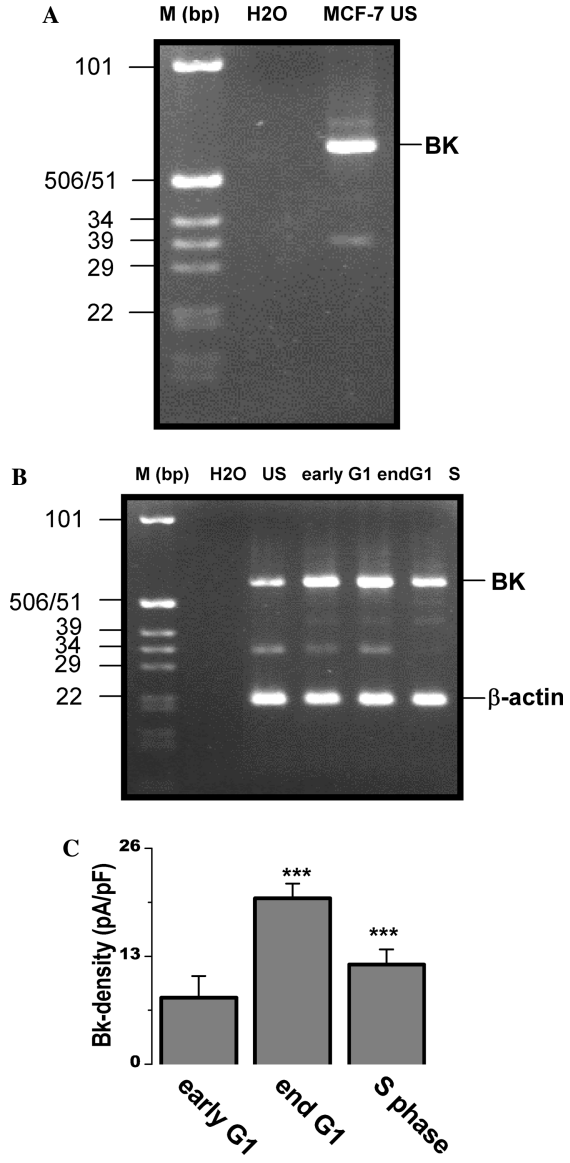

Fig. 3. Modulation of the BK potassium channel during the cell cycle in MCF-7 cells. (A) RT-PCR studies of hBK mRNA expression in the MCF-7 cells during the cell cycle. Expression of BK mRNA in MCF-7 cells. For the expression study of BK, total RNAs of MCF-7 cells were reverse transcribed, followed by PCR using MCF-7 cell cDNA (100 ng RNA equivalents) and specific primers amplifying BK (598 bp) as described in Materials and methods. H_2O and samples without reverse transcriptase (−RT) were used as negative controls. Amplified fragments were resolved by 1.5% agarose-gel electrophoresis and visualized by EtBr staining. M, molecular weight marker. (B) Variation of BK mRNA expression during the cell cycle. MCF-7 cells were synchronized in early G1, end G1, and S phases as described in Materials and methods. After RNA extraction and reverse transcription, equal amounts of the cDNA (20 ng RNA equivalents) from unsynchronized cells (US) or synchronized cells were used to amplify BK and β-actin (227 bp) by PCR. (C) BK current-density in cells arrested in early G1, late G1, and in the S phases. BK current-density was determined by dividing the r-IbTX-sensitive current by the membrane capacitance. I_{BK}-density increased in cells arrested in late G1 and in the S phases. The data represent means ± SD. The experimental group medians marked by asterisks are significantly different from the control median ($p < 0.001$).

G1 progression. Inhibition of the hEAG K^+ channel induced a depolarization of membrane potential and arrested cells in the early G1 phase [7]. In this work, we studied the functional role of BK channels in controlling the membrane potential of MCF-7 cells throughout the cell cycle. We performed current-clamp experiments on each group of cells and determined the resting membrane potential. Application of 50 nM r-IbTX did not produce depolarization in cells arrested in the early G1 phase (Fig. 4A). However, r-IbTX induced a depolarization of 8 ± 3 mV ($n = 11$) and 12 ± 4 mV ($n = 10$) in cells arrested at the end of G1 and S, respectively (Fig. 4A). Similar results were obtained with the ChTX perfusion (data not shown). Treatment of MCF-7 cells arrested in the early G1 with ionomycin (1 μM) induced a pronounced hyperpolarization (Fig. 4B). Extracellular perfusion of r-IbTX (50 nM) induced a slight depolarization in ionomycin-induced hyperpolarization (Fig. 4B).

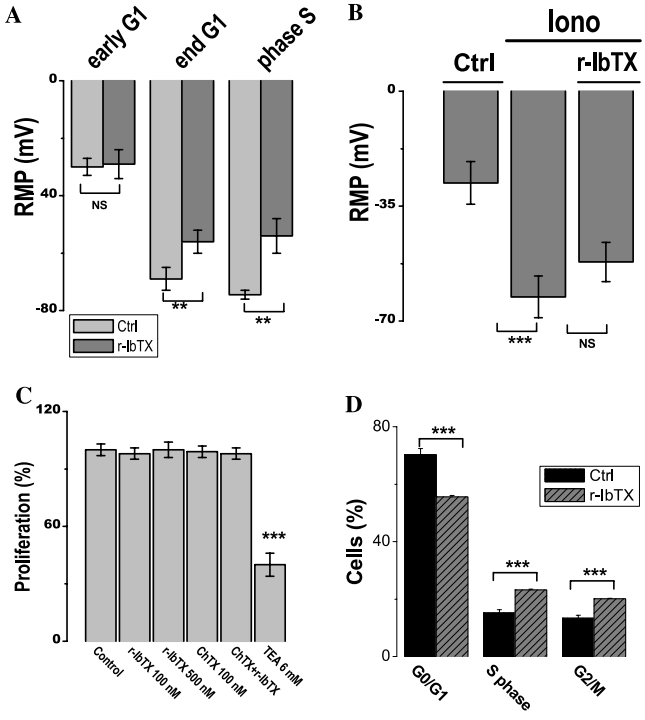

Fig. 4. Effect of BK channel blockers on the resting membrane potential, cell proliferation, and cell cycle. All bath solutions contained 50 nM α-dendrotoxin to block Kv1.1 K^+ channels. (A) RMP distribution of cells accumulated in early G1, late G1, and S phases. An extracellular perfusion of r-IbTX (50 nM) induced only a 10 mV depolarization in cells accumulated in late G1 and S phases. (B) In cells arrested in the early G1, extracellular perfusion with ionomycin induced hyperpolarization of the membrane potential. Extracellular perfusion of r-IbTX (50 nM) induced a slight inhibition of hyperpolarization induced by ionomycin. $^{**}p < 0.01$, $^{***}p < 0.001$. (C) Effect of r-IbTX, ChTX, and TEA on MCF-7 cell proliferation. The bars represent six independent experiments ± SD. (D) Cell-cycle analysis, cells were incubated in culture medium with r-IbTX (500 nM) for 4 days. r-IbTX induced a significant increase in cells arrested in the S phase and a decrease in cells arrested in the G1 phase. The experimental group medians marked by asterisks are significantly different from the control median ($^{***}p < 0.001$).

Proliferation and cell-cycle analysis

We also investigated the effect of r-IbTX, ChTX alone or combined and TEA (6 mM) as a positive control on MCF-7 cell proliferation. The MCF-7 cell proliferation was estimated by cell proliferation assay kit, 4 days after drug application (see Materials and methods). r-IbTX (100 and 500 nM), ChTX (100 nM) ChTX, r-IbTX, and the two toxins combined had no effect on cell proliferation (Fig. 4C). Only TEA (6 mM) inhibited the cell proliferation by $68 \pm 2\%$ (Fig. 4C).

Recently, it has been reported that the BK channels may contribute to the maintenance of DNA synthesis [29]. To test this hypothesis, we analyzed the cell cycle using a flow cytometry technique after 4 days in culture in the presence of r-IbTX (500 nM). Exponentially growing cells had a distribution of $70 \pm 2.06\%$ in G1, $15.16 \pm 1.13\%$ in S, and $13.33 \pm 1.08\%$ in G2/M (n = 6). In r-IbTX-treated cells, the proportion of G1 cells decreased significantly to $55.6 \pm 0.5\%$ ($n = 6$, $p < 0.001$), while there was a significant increase in S-phase cells ($23.16 \pm 0.26\%$, $n = 6$, $p < 0.001$) and G2–M phase ($20.1 \pm 0.17\%$, Fig. 4D).

Discussion

Ca^{2+}-activated K^+ channels expressed in MCF-7 cells

Wegman et al. [12] have previously reported that the MCF-7 cell line expresses a 23-pS Ca^{2+} and voltage-activated K^+ conductance. Our experiments demonstrate that the MCF-7 cell line expresses Ca^{2+}-activated K^+ channels. The identification of the current as a BK current is based on the pharmacological and molecular profile. The BK channel expressed in MCF-7 cells was voltage-dependent and blocked by r-IbTX, ChTX, TEA, and when Cs was applied internally.

Cell-cycle variation of the BK channels

One important result of this study is that the expression rate and the density of the BK channel changed markedly during the cell cycle, as estimated from determinations by the whole cell and RT-PCR techniques. The BK current-density and the mRNA transcript seemed to be largest at the end of the G1 phase, thus suggesting that synthesis of BK proteins may underlie the up-regulation of functional BK channels. On the other hand, BK mRNAs were found in cells arrested in early G1, suggesting that the pre-existing BK channels were probably inactive due to low $[Ca^{2+}]_i$. Figs. 1C and D illustrate the activation of BK currents in MCF-7 cells

arrested in early G1 by the increase in $[Ca^{2+}]_i$. Moreover, both BK-density and mRNA levels decreased in the S phase.

Direct links between channel activity and particular stages of the cell cycle have been reported [1]. In cultured MCF-7 cells, inhibition of BK Ca^{2+}-activated channels induced an accumulation in the S phase. This result suggested that this channel may contribute to the mechanism or mechanisms that regulate DNA synthesis. Indeed, Kodal et al. [29] have reported that in Müller cells, the inhibition of the activity of BK channels with TEA or by IbTX had no effect on the DNA synthesis at normal extracellular K^+, but reduced the rate of DNA synthesis either after the application of the EGF or at higher extracellular K^+. They suggested that BK channels may contribute to the maintenance of DNA synthesis by increasing mitogen-induced increase in intracellular Ca^{2+} concentration. Moreover, Moll et al. [30] have also reported in the Müller glial cells that BK channels are involved in the ATP-induced stimulation of DNA synthesis.

BK K^+ channels and cell proliferation

Several studies have pointed to a controversial role of BK channels in cell proliferation. Thus, blocking BK channel activity by IbTX or ChTX, in control conditions; i.e., low extracellular K^+, has no effect on astrocytoma or meningioma cell growth [31–33] therefore suggesting that Ca^{2+}-activated K^+ channels do not contribute to the proliferative response of these cells. However, astrocytoma cell proliferation can be completely abolished by IbTX under high extracellular K^+ conditions [31]. Retinal glial cells obtained from diseased retina (proliferative retinopathy) show an increased expression of BK channels, suggesting a correlation between BK channel expression and proliferation [34]. Moreover, in human keratinocyte cells, the BK channels contribute to the resting potential which may control the Ca^{2+} influx and thereby their proliferation and differentiation [35].

Treating MCF-7 cells with BK-inhibitors (r-IbTX or ChTX) induced a weak depolarization and a lack of effect on cell proliferation. One explanation is that BK channel activation seems to play either a minor or no role at all in MCF-7 cell membrane hyperpolarization and thus does not affect the cell proliferation. Indeed, hyperpolarization is essential for proliferation as shown by the inhibitory effect of K^+ channel antagonists on the growth of many different cell types including MCF-7 cells [1,7], endothelial cells [36], Schwann cells [37], and T cells [38]. However, the absence of r-IbTX effect on cell proliferation may suggest that, under resting conditions, the intracellular free Ca^{2+} is too low to activate r-IbTX-sensitive, Ca^{2+}-activated K^+ channels. This conclusion is in agreement with the results of de-Allie et al. [39] showing that Ca^{2+}-activated K^+ channels are inactive in the presence of a basal cytosolic Ca^{2+} of 42 nM. We found that intracellular $[Ca^{2+}]$ levels were lower in the MCF-7 arrested in the early G1 phase (48.6 ± 5.6 nM, $n = 24$).

Furthermore, the failure of BK channels to block proliferation was perhaps due to the binding of these peptide toxins (r-IbTX and ChTX) to serum proteins. Indeed, it was reported that the serum affected the inhibition of proliferation by the peptide toxin [40].

BK K^+ channels, membrane potential, and cell proliferation

In the breast cancer MCF-7 cell line, we and others have reported that both the control of proliferation and the cell-cycle progression depend on K^+ channel activity according to the "membrane potential" model [1,7]. Thus, K^+ channel blockers which depolarized the membrane potential inhibited proliferation [1]. BK K^+ channels seem slightly involved in the regulation of the membrane potential, although only at the end G1 and S phases, when the BK current-density increased (Fig. 3C). This increase in the BK current-density might be due to a serum effect. Indeed, serum and growth factors have been reported to up-regulate K^+ channels in human myeloblastic cells [41]. As MCF-7 cells express numerous K^+ channels, serum could activate some of them thereby inducing a sufficient hyperpolarization which could stimulate cell proliferation. In MCF-7 cells, serum starvation induced an inhibition of cell proliferation, cell arrest in the G1 phase, and a membrane depolarization [7]. Thus, the lack of the r-IbTX effect on the membrane potential and on cell proliferation suggests that the membrane potential was mainly determined by another K^+ channel type.

Moreover, Ca^{2+}-activated K^+ channels have been shown to participate in volume regulation and migration [42,43]. In human glioma cells, TEA (at concentrations that selectively inhibit BK channels, i.e., <1 mM) reduced migration [44]. More recently, Kraft et al. [45] reported that the potent activator of BK channels in 1321N1 human glioma cells inhibits cell migration. At this time, the physiological role of BK expression, which does not considerably contribute to MCF-7 hyperpolarization, remains unclear and requires further studies in order to satisfactorily understand it. However, we do not exclude a role of the BK K^+ channels in volume regulation, migration or angiogenesis in breast cancer cells.

In conclusion, we argue that MCF-7 expresses a different pool of K^+ channels, including BK^+ channels. Under our control conditions, BK channel did not appear to be involved in MCF-7 cell proliferation. However, BK channel activity is linked to cell-cycle progression.

Acknowledgments

This work was supported by the Région Nord-Pas de Calais, the Ministère de l'Education Nationale de l'Enseignement Supérieur et de la Recherche, INSERM, and l'Association de la Recherche contre le Cancer (ARC, France). We are indebted to N. Jouy for excellent technical assistance.

References

[1] W.F. Wonderlin, J.S. Strobl, J. Membr. Biol. 154 (1996) 91–107.
[2] C. Deutsch, M. Price, S. Lee, V.F. King, M.L. Garcia, J. Biol. Chem. 266 (1991) 3668–3674.
[3] R. Chittajallu, Y. Chen, H. Wang, X. Yuan, C.A. Ghiani, T. Heckman, C.J. McBain, V. Gallo, Proc. Natl. Acad. Sci. USA 99 (2001) 2350–2355.
[4] M.L. Day, S.J. Pickering, M.H. Johnson, D.I. Cook, Nature 365 (1993) 560–562.
[5] M.L. Day, M.H. Johnson, D.I. Cook, EMBO J. 17 (1998) 1952–1960.
[6] A. Czarnecki, L. Dufy-Barbe, S. Huet, M.F. Odessa, L. Bresson-Bepoldin, Am. J. Physiol. Cell Physiol. 284 (2003) C1054–C1064.
[7] H. Ouadid-Ahidouch, X. LeBourhis, M. Roudbaraki, R.A. Toillon, P. Delcourt, N. Prevaskaya, Receptors Channels 7 (2001) 345–356.
[8] H. Ouadid-Ahidouch, F. Chaussade, M. Roudbaraki, C. Slomianny, E. Dewailly, P. Delcourt, N. Prevarskaya, Biochem. Biophys. Res. Commun. 278 (2000) 272–277.
[9] M. Abdul, A. Santo, N. Hoosein, Anticancer Res. 23 (2003) 3347–3351.
[10] D. Mu, L. Chen, X. Zhang, L.H. See, C.M. Koch, C. Yen, J.J. Tong, L. Spiegel, K.C. Nguyen, A. Servoss, Y. Peng, L. Pei, J.R. Marks, S. Lowe, T. Hoey, L.Y. Jan, W.R. McCombie, M.H. Wigler, S. Powers, Cancer Cell 3 (2003) 297–302.
[11] E. Klimatcheva, W.F. Wonderlin, J. Membr. Biol. 171 (1999) 35–46.
[12] E.A. Wegman, J.A. Young, D.I. Cook, Pflügers Arch. 417 (1991) 562–570.
[13] J.S. Strobl, W.F. Wonderlin, D.C. Flynn, Gen. Pharmacol. 26 (1995) 1643–1649.
[14] H. Ouadid-Ahidouch, X. Lebourhis, R.A. Toillon, N. Prevarskaya, J. Physiol. 523 (1998) P158.
[15] C. Vergara, R. Latorre, N.V. Marrion, J.P. Adelman, Curr. Opin. Neurobiol. 8 (1998) 321–329.
[16] C. Miller, E. Moczydlowski, R. Latorre, M. Phillips, Nature 313 (1985) 316–318.
[17] R. Khanna, M.C. Chang, W.J. Joiner, L.K. Kaczmarek, L.C. Schlichter, J. Biol. Chem. 274 (1999) 4838–14849.
[18] N.J. Rush, Y. Liu, K.A. Pleyte, Clin. Exp. Pharmacol. Physiol. 23 (1996) 1077–1082.
[19] L. Catacuzzeno, D.A. Pisconti, A.A. Harper, A. Petris, F. Franciolini, Pflügers Arch. 441 (2000) 208–218.
[20] N.J. Rush, R.G. De Lucena, T.A. Wooldridge, S.K. England, A.W. Cowley, Hypertension 19 (1992) 301–307.
[21] J.J. Liu, J. Chao, M.C. Jiang, S.Y. Ng, J.J. Yen, H.F. Yang-Yen, Mol. Cell. Biol. 15 (1995) 3654–3663.
[22] C.B. Ransom, H.J. Sontheimer, J. Neurophysiol. 85 (2001) 790–803.
[23] M. Partiseti, D. Choquet, A. Diu, H. Korn, J. Immunol. 148 (1992) 3361–3368.
[24] C.S. Lin, R.C. Boltz, J.T. Blake, M. Nguyen, A. Talento, P.A. Fischer, M.S. Springer, N.H. Sigal, R.S. Slaughter, M.L. Garcia, G.J. Kaczorowski, G.C. Koo, J. Exp. Med. 177 (1993) 637–645.
[25] X.F. Dong, Y. Berthois, C. Dussert, D. Isnardon, J. Palmari, P.M. Martin, Anticancer Res. 12 (1992) 2085–2092.
[26] P. Chomczynski, N. Sacchi, Anal. Biochem. 162 (1987) 156–159.
[27] S. Wang, Z. Melkoumian, K.A. Woodfork, C. Cather, A.G. Davidson, W.F. Wonderlin, J.S. Strobl, J. Cell. Physiol. 176 (1998) 456–464.
[28] K. Keyomarsi, L. Sandoval, V. Band, A.B. Pardee, Cancer Res. 51 (1991) 3602–3609.
[29] H. Kodal, M. Weick, V. Moll, B. Biedermann, A. Reichenbach, A. Bringmann, Invest. Ophthalmol. Vis. Sci. 41 (2000) 4262–4267.
[30] V. Moll, M. Weick, I. Milenkovic, H. Kodal, A. Reichenbach, A. Bringmann, Invest. Ophthalmol. Vis. Sci. 43 (2002) 766–773.
[31] D. Basrai, R. Kraft, C. Bollensdorff, L. Liebmann, K. Benndorf, S. Patt, Neuroreport 13 (2002) 403–407.
[32] L.S. Chin, C.C. Park, K.M. Zitmay, M. Sinha, A.J. Dipatri, P. Perillan, J.M. Simard, J. Neurol. Res. 48 (1997) 122–127.
[33] R. Kraft, K. Benndorf, S. Patt, J. Membr. Biol. 175 (2000) 25–33.
[34] A. Bringmann, M. Francke, T. Pannicke, B. Biedermann, H. Kodal, F. Faude, W. Reichelt, A. Reichenbach, Glia 29 (2000) 35–44.
[35] V.H. Nguyen, F. Markwardt, Exp. Dermatol. 11 (2002) 319–326.
[36] J. Wiecha, B. Munz, Y. Wu, T. Noll, H. Tillmanns, B. Waldecker, J. Vasc. Res. 35 (1998) 363–371.
[37] A. Sobko, A. Peretz, O. Shirihai, S. Etkin, V. Cherepanova, D. Dagan, B. Attali, J. Neurosci. 18 (1998) 10398–10408.
[38] B.S. Jensen, N. Odum, N.K. Jorgensen, P. Christophersen, S.P. Olesen, Proc. Natl. Acad. Sci. USA 96 (1999) 10917–10921.
[39] F.A. de-Allie, S.R. Bolsover, A.V. Nowicky, P.N. Strong, Br. J. Pharmacol. 117 (1996) 479–487.
[40] B.D. Freedman, M.A. Price, C.J. Deutsch, J. Immunol. 149 (1992) 3784–3794.
[41] L. Wang, B. Xu, E.R. White, L. Lu, Am. J. Physiol. 273 (1997) C1657–C1665.
[42] H. Parantes-Morales, R.A. Murray, L. Lilja, J. Moran, Am. J. Physiol. Cell Physiol. 66 (1994) C165–C171.
[43] A. Schwab, B. Schuricht, P. Seeger, J. Reinhardt, P.C. Dartsch, Pflügers Arch. 438 (1999) 330–337.
[44] L. Soroceanu, T.J. Manning, H.J. Sontheimer, J. Neurosci. 19 (1999) 5942–5954.
[45] R. Kraft, P. Krause, S. Jung, D. Basrai, L. Liebmann, J. Bolz, S. Patt, Pflugers Arch. 446 (2003) 248–255.